THE JOURNAL OF PHYSICAL CHEMISTRY A
Article
pubs.acs.org/JPCA

Numerical Simulation of the Kinetics of Radical Decay in Single-Pulse High-Energy Electron-Irradiated Polymer Aqueous Solutions

Björn Dahlgren,[†] Clelia Dispenza,[‡,§] and Mats Jonsson*[,†]

[†]Department of Chemistry, KTH Royal Institute of Technology, SE-100 44 Stockholm, Sweden
[‡]Dipartimento di Ingegneria, Università degli Studi di Palermo, Viale delle Scienze 6, 90128 Palermo, Italy
[§]Istituto di Biofisica (IBF), Consiglio Nazionale delle Ricerche, Via Ugo La Malfa 153, 90146 Palermo, Italy

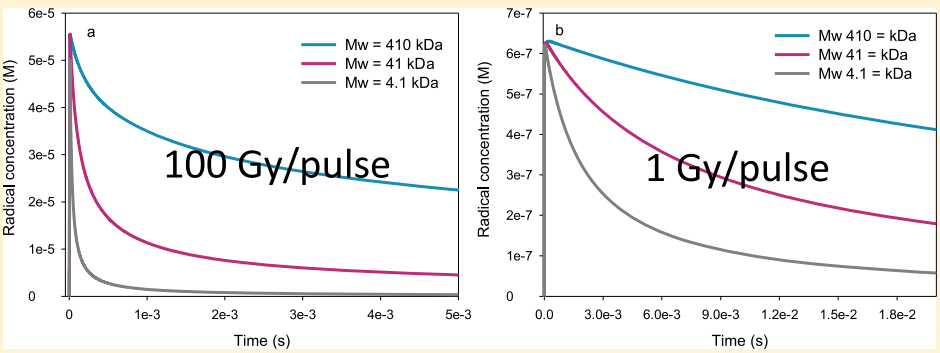

ABSTRACT: A new method for the numerical simulation of the radiation chemistry of aqueous polymer solutions is introduced. The method makes use of a deterministic approach combining the conventional homogeneous radiation chemistry of water with the chemistry of polymer radicals and other macromolecular species. The method is applied on single-pulse irradiations of aqueous polymer solutions. The speciation of macromolecular species accounts for the variations in the number of alkyl radicals per chain, molecular weight, and number of internal loops (as a consequence of an intramolecular radical−radical combination). In the simulations, the initial polymer molecular weight, polymer concentration, and dose per pulse (function of pulse length and dose rate during the pulse) were systematically varied. In total, 54 different conditions were simulated. The results are well in line with the available experimental data for similar systems. At a low polymer concentration and a high dose per pulse, the kinetics of radical decay is quite complex for the competition between intra- and intermolecular radical−radical reactions, whereas at a low dose per pulse the kinetics is purely second-order. The simulations demonstrate the limitations of the polymer in scavenging all the radicals generated by water radiolysis when irradiated at a low polymer concentration and a high dose per pulse. They also show that the radical decay of lower-molecular-weight chains is faster and to a larger extent dominated by intermolecular radical−radical reactions, thus explaining the mechanism behind the experimentally observed narrowing of molecular weight distributions.

INTRODUCTION

Radical−radical reactions between macromolecular species constitute the major route for termination in free radical polymerization. The kinetics of these reactions is therefore a key to the understanding of radical polymerization and the optimization of polymeric products, in terms of their chemical composition, molecular weight, and topology. In addition, radical−radical combination is an important reaction in polymer cross-linking as well as in the synthesis of hydrogels and nanogels. Nanogels, in particular, have recently raised considerable interest in the biomedical field, because of their diverse applications in tissue engineering, regenerative medicine, and drug delivery.[1,2] Furthermore, free radical formation has been observed in proteins because of oxidative stress, UV, or ionizing irradiation exposure. Their formation, via direct and indirect mechanisms, and follow-up reactions, including dimerization, polymerization, cross-linking, polypeptide chain scission, and disruption of labile amino acid residues, are implicated in the pathogenesis of several pathologies, including cancer, aging, and atherosclerosis.[3−5]

Direct measurements of the kinetics of radical−radical reactions in solution are usually performed using pulse radiolysis or laser flash photolysis. Both methods are based on time-resolved detection of the radical species after initiation using either an electron pulse or a laser pulse. In the former case, the radical initiation is achieved through reactions between primary radiolysis products of the solvent and solutes, whereas in the latter case direct photolysis of a solute precursor is used. For water-soluble polymers (and other macromolecules), pulse radiolysis can be particularly useful as the radiation chemistry of water is very well known and numerous experimental studies can be found in the literature.[3,6−21] Upon

Received: April 1, 2019
Revised: May 11, 2019
Published: May 29, 2019

DOI: 10.1021/acs.jpca.9b03013
J. Phys. Chem. A XXXX, XXX, XXX−XXX

exposure to γ-photons or accelerated electrons, water is decomposed into $^{\bullet}OH$ (0.28 μmol J^{-1}), $H^{\bullet}$ (0.062 μmol J^{-1}), e_{aq}^{-} (0.28 μmol·J^{-1}), H_2 (0.047 μmol·J^{-1}), H_2O_2 (0.073 μmol·J^{-1}), and H_3O^+ (0.28 μmol·J^{-1}). Numbers in parentheses indicate the radiation chemical yield or *G*-value of each radiolysis product.[22] Radical sites on the polymer are formed upon hydrogen abstraction by $^{\bullet}OH$ and $H^{\bullet}$. By saturating the aqueous solution with N_2O, the strongly reducing hydrated electron can be converted into a hydroxyl radical. This increases the yield of the formed polymer radicals.[22] Under certain conditions, pulse radiolysis of aqueous polymer solutions can lead to the formation of multiple radical sites on the same chain. The conditions that favor the formation of multiple radical sites on the same chain are high doses per pulse (high initial radical concentration) and low polymer concentrations. In such a case, both intra- and intermolecular radical−radical reactions become possible and the subsequent kinetic analysis is more complex as simple second-order kinetics can no longer be applied. The kinetics is initially dominated by intramolecular radical−radical reactions but eventually, as the number of radical sites per chain decrease, intermolecular radical−radical reactions will also occur. This can appear as if an overall rate constant for the process consuming the radicals in the system is changing with time and therefore dispersive kinetics is often used to analyze these systems.[23]

The conditions favoring intramolecular radical−radical reactions have been employed in the radiation synthesis of nanogels from polymer aqueous solutions.[24−28] Interestingly, the conditions that favor intramolecular radical−radical reactions coincide with the conditions when scavenging of the primary radicals formed in the radiolysis of water is no longer quantitative. Under these conditions, a fraction of the hydroxyl radicals can recombine and produce hydrogen peroxide. This can have a significant influence on the further reactions in the system. In systems exposed to continuous irradiation or a sequence of pulses, the formation of H_2O_2 will eventually lead to the production of O_2.[29]

It is therefore desirable to be able to perform numerical simulations on the system both in order to confirm mechanistic and kinetic data and to be used as a predictive tool for process optimization. The obvious first step in the development of such a modeling tool is simulation of single-pulse irradiations or a typical pulse radiolysis experiment.

Numerical simulations of homogeneous radiation chemistry have been performed with high accuracy for decades. However, simulations taking into account also the chemistry of macromolecules in irradiated aqueous systems are considerably scarcer in the literature.

In this work we present a new approach for modeling the radiation chemistry of aqueous solutions containing polymers. The method is used to simulate the systems exposed to a single pulse of electrons. In the simulations we explore the effects of dose per pulse, concentration of polymer, and polymer molecular weight on the kinetics of polymer radical decay. The results are discussed in view of previous experimental observations.

MODEL DESCRIPTION

The numerical simulations are based on a deterministic approach encompassing the conventional homogeneous radiation chemistry of water as well as chemical reactions involving polymer chains and polymer radicals. To connect the radiation chemistry of water to the chemistry of the polymer species in single-pulse irradiations, the following reactions are included (in addition to the standard set of reactions for water radiolysis):

- Reactions between primary radiolysis products ($^{\bullet}OH$ and $H^{\bullet}$) and macromolecular species.
- Inter- and intramolecular radical−radical reactions of alkyl radicals.

The multitude of possible reactions in the macromolecular system is handled by allowing a fairly large number of macromolecular species.

Speciation. In general, an irradiated aqueous polymer solution soon becomes a very complex reaction system. Even if we start with a monodisperse polymer, we soon end up with a number of different first-generation products, which in turn will lead to an even larger number of second-generation products and so on. To be able to handle such a reaction system we must use quite a large number of chemical species. In a general model for continuous irradiation or irradiation using sequences of pulses, speciation of macromolecular species can be done by taking into account the size of the macromolecule (i.e., number of segments) (n), the number of alkyl radicals per chain (a), the number of oxyl radicals per chain (o), and the number of internal loops (l) (stemming from intramolecular radical−radical combination). However, when simulating single-pulse irradiation at fairly low doses and for solutions that are initially free from molecular oxygen, we can limit the speciation to account for only the size (n), the number of alkyl radicals per chain (a), and the number of internal loops (l). The original size of the macromolecular species in our model has by default an initial value of 100. It is worth pointing out that the "size" is directly connected to polymer molecular weight and not to the radius of gyration or the hydrodynamic radius of the chain. To keep the number of possible macromolecular species at a level that can be handled with reasonable computational time, only a limited number of states are allowed within each category. Every unique combination of allowed states of the different categories used defines one species. The reactions of relevance are depicted below.

$$P + xOH^{\bullet} \rightarrow P^{x\bullet} \quad \text{hydrogen abstraction} \quad (1a)$$

$$P + xH^{\bullet} \rightarrow P^{x\bullet} \quad \text{hydrogen abstraction} \quad (1b)$$

$$P^{x\bullet} \rightarrow P^{(x-2)\bullet} \quad \text{intramolecular crosslinking} \quad (2)$$

$$P^{x\bullet} \rightarrow P^{(x-2)\bullet}(=) \quad \text{intramolecular disproportionation} \quad (3)$$

$$P^{x\bullet} \rightarrow P^{y\bullet} \rightarrow P - P^{(x+y-2)} \quad \text{intermolecular crosslinking} \quad (4)$$

$$P^{x\bullet} + P^{y\bullet} \rightarrow P^{(x-1)\bullet}(=) + P^{(y+1)\bullet} \quad \text{intermolecular disproportionation} \quad (5)$$

The speciation is defined in Table 1. The starting point is **a**, which is the original polymer chain. Upon reaction with $^{\bullet}OH$ or $H^{\bullet}$, an alkyl radical, **b**, is formed. The alkyl radical can react in several different ways. In this particular example, we have the reaction with another $^{\bullet}OH$ or $H^{\bullet}$ to produce a chain with two alkyl radical sites, **c**; the reaction with another radical of the same type to produce the dimer, **e**; and the intramolecular

DOI: 10.1021/acs.jpca.9b03013
J. Phys. Chem. A XXXX, XXX, XXX−XXX

Table 1. Definition of the Species a−e in Reaction 1a−5

species	n	a	l	notation
a	100	0	0	$n_{100}a_0l_0$
b	100	1	0	$n_{100}a_1l_0$
c	100	2	0	$n_{100}a_2l_0$
d	100	0	1	$n_{100}a_0l_1$
e	200	0	0	$n_{200}a_0l_0$

combination of the two alkyl radical sites on **c** to produce an internal loop, **d**.

The combination between two alkyl radicals always competes with disproportionation to produce an alkane and an alkene, leaving the size of the molecules unchanged. It should be noted that the speciation system used here does not include double bonds. This means that disproportionation is included in the model for its effects on polymer "size" but not for its effects on polymer chemical composition.

As many of the radical-bearing chains can undergo a multitude of intra- and intermolecular radical−radical reactions the number of reactions included in the simulation becomes several orders of magnitude higher than the number of defined macromolecular species.

Furthermore, the method used for speciation does not account for site specificity either. Indeed, an alkyl radical can be formed at any position and the outcome of the subsequent reactions will largely depend on its site. Allowing for site specificity would lead to an explosion in the size of the system of equations that would be very difficult to handle from a computational point of view.

Kinetics. For each class of reactions considered (i.e., 1a−5 above) we assign a rate constant (based on literature data), and an expression for how the rate constant depends on the properties of the participating macromolecule(s).

For reaction 1a (hydrogen abstraction, which we will specifically refer to as "1a" in the case of the hydroxyl radical) we assign (based on Figure 3, p 478 in ref 30): $k_{1a} = \left(\frac{n}{n_0}\right)^{s_{\text{inter-}n}} k_{OH}$, where n/n_0 is the relative length of the chain, $s_{\text{inter-}n} = -0.3$ is a scaling factor which we extract from the regression in the aforementioned figure, and k_{OH} is chosen such that $k_{1a} = 1.3 \times 10^9$ M^{-1} s^{-1} for a molecular weight of 1 kDa (so that it reproduces the data in the aforementioned figure).

For reaction 1b (hydrogen abstraction by a hydrogen atom), we assign the same rate expression as for reaction 1a, but divided by a factor of 102 (which is the ratio between OH/H rate constants for *c*-hexane according to refs[31,32]).

For intramolecular cross-linking, that is reaction 2, we assign an expression for the rate constant as

$$k_2 = \left(\frac{a}{2}\right)^{s_{\text{intra-r}}} \left(\frac{n}{n_0}\right)^{s_{\text{intra-}n}} P_d \cdot k_{\text{rad-rad-intra}}$$

where a is the number alkyl radicals on the chain, $s_{\text{intra-r}} = 2.719$ is a scaling factor for intramolecular polymer−radical reactions which was derived from the slopes of the regression lines in Figure 8, p 863 in ref 23, $s_{\text{intra-}n} = -2.0625$ is a length scaling factor which was also extracted from the vertical spacing between the regression lines in the same figure, $k_{\text{rad-rad-intra}} = \left(\frac{M_W(\text{polymer})}{M_W(\text{monomer})}\right)^{s_{\text{intra-}n}} \frac{\ln 2}{T_{1/2}}$ is the first-order rate constant for intramolecular radical−radical reactions (for the case of only two radicals per polymer chain) and is expressed in terms of $T_{1/2}$ (loop closure) = 8×10^{-5} s (taken from Figure 17, p 867, ref 33 but scaled down here by a factor of 100 to adapt to this system), and $P_d = 0.38$ (from p 150, ref 34) is the probability of disproportionation (vs combination).

Reaction 3 is assigned the same expression as 2 with the difference that we apply the probability for disproportionation instead of its complement ($k_3 = \frac{P_d}{(1-P_d)} k_2$).

For reaction 4 (intermolecular cross-linking) we set

$$k_4 = (1 - P_d)\frac{a\underline{a}n_0^2}{n\underline{n}} k_{\text{alkyl-inter}}$$

where the underlined variables correspond to values from the second chain, $k_{\text{alkyl-inter}}$ = is 2.5×10^7 M^{-1} s^{-1} (based on Figure 5, p 182, ref 34), and the form of the expression is chosen so that the rate constant is proportional to the number of alkyl radicals on each chain, and inversely proportional to the respective chain length (the ratio a/n is in a sense the "alkyl-radical concentration" on the polymer, a metric which should reasonably correlate with the observed rate of reaction between two such polymers). This is also the expression used for reaction 5 (intermolecular disproportionation) but with the probability for disproportionation used instead of its complement ($k_5 = \frac{P_d}{(1-P_d)} k_4$).

Admittedly, the actual position of radical sites plays a major role for the kinetics of a radical−radical reaction. As this cannot be accounted for in the present approach, the rate constants and the corresponding scaling represent mean values of the possible situations.

Simulation Conditions. The simulations were performed using polymer molecular weights of 410, 41, and 4.1 kDa. The polymer concentrations expressed as mass fractions were 0.1, 0.01, and 0.001. The dose rate during the pulse was 1.0×10^7 Gy s^{-1} and the pulse lengths were 10^{-7}, 10^{-6}, and 10^{-5} s corresponding to 100, 10, and 1 Gy per pulse, respectively. A complete parallel set of simulations, using a dose rate during the pulse of 2.0×10^7 Gy s^{-1}, was also performed. In total, simulations of 54 different conditions were performed.

The output from the simulations is the total alkyl radical concentration as a function of time. This is to allow direct comparison to pulse radiolysis data where the observed absorbance is usually attributed to the total radical concentration regardless of radical location.

COMPUTATIONAL DETAILS

A system of ordinary differential equations is formulated based on the chemical reactions. A self-contained archive of the source code, its dependencies, and the tools needed to run the code can be found in ref 35.

The initial value problem is then solved numerically as a function of time for each given pulse sequence. We used the CVodes solver from the SUNDIALS program suite,[36] and as the problem was stiff, we used the BDF method together with an analytic Jacobian. The rate expressions are conventionally derived from the law of mass action, but as our model is coarse-grained (in the sense that there are large steps between allowed values of the state variables describing the species in our ensemble), we need to generate a consistent set of stoichiometries and rates for all possible reactions. The allowed states were as follows

DOI: 10.1021/acs.jpca.9b03013
J. Phys. Chem. A XXXX, XXX, XXX−XXX

$$n = \{10,\ 100,\ 200,\ 600,\ 2400\}$$

$$a = \{0,\ 1,\ 2,\ 6,\ 24,\ 120\}$$

$$l = \{0,\ 1,\ 2,\ 6,\ 24\}$$

Depending on the allowed states, some reactions will be trivial to formulate. For example, the reaction of the hydroxyl radical with a polymer chain, formed by 100 segments bearing only one radical ($n_{100}a_1l_0$), which forms a chain with the same length bearing two radial sites ($n_{100}a_2l_0$) and water can be described as

$$n_{100}a_1l_0 + {}^{\bullet}\mathrm{OH} \rightarrow n_{100}a_2l_0 + \mathrm{H_2O}$$

This is a reaction where both the macromolecular reactant and product are allowed states. When this is not the case, an effective average based on a linear combination of allowed states must be used. For example, the product of a further reaction of $n_{100}a_2l_0$ with a hydroxyl radical cannot be expressed as $n_{100}a_3l_0$ as $a = 3$ in not an allowed state, then the reaction products are expressed as

$$n_{100}a_2l_0 + {}^{\bullet}\mathrm{OH} \rightarrow 3/4\ n_{100}a_2l_0 + 1/4\ n_{100}a_6l_0 + \mathrm{H_2O}$$

RESULTS AND DISCUSSION

Previous experimental studies on the radiation chemistry of dilute aqueous polymer solutions have both directly and indirectly shown that the conversion of H-abstracting radicals into polymer radicals is not quantitative at low polymer concentrations.[14,29,37] In ref 14, this is illustrated by polymer concentration-dependent spectral differences whereas in refs[29,37] the nonquantitative conversion is illustrated by increased formation of H_2O_2 at lower polymer concentrations. In Figure 1, we have plotted the scavenging capacity, expressed

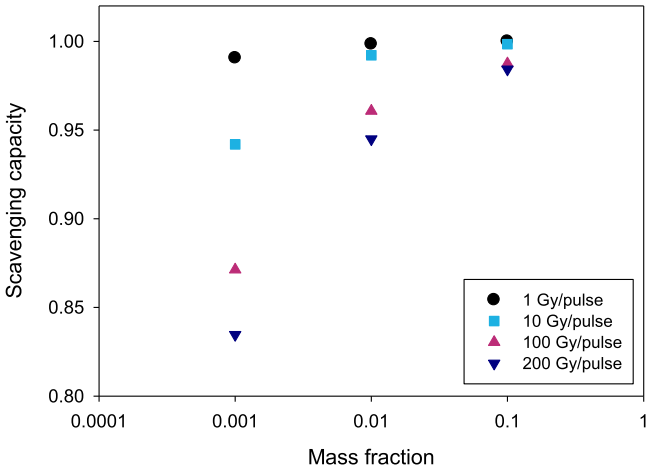

Figure 1. Scavenging capacity plotted against polymer concentration for four different doses per pulse (the initial molecular weight is 410 kDa).

as the fraction between the actual maximum concentration of alkyl radicals from the simulated single-pulse irradiation of a polymer with 410 kDa and the theoretical maximum concentration (calculated from the dose per pulse and the G-values $^{\bullet}$OH and H$^{\bullet}$) as a function of polymer concentration (mass fraction) for four different doses per pulse. In previous experiments the dose per pulse ranges from a few Gy to several hundred Gy.[13,14] The dose range used in the simulations overlaps with the experimental range. The maximum concentration of alkyl radicals from the simulations is a measure of the total number of alkyl radical sites per dm^3, that is, it includes also multiple sites on the same chain. It simulates pulse radiolysis experiments carried out with polymers characterized by only one possible type of radical structure, for example polyethyleneoxide, where the measured transient absorbance is proportional to the total radical concentration regardless of radical location.

As can be seen in the figure, the scavenging capacity depends both on the polymer concentration and on the dose per pulse, just as expected. For the highest polymer concentration, the scavenging capacity is quite close to 100% regardless of the dose per pulse (in the range of 1−200 Gy). However, at the lower polymer concentrations the scavenging capacity deviates significantly from 100% and clearly decreases with increasing the dose per pulse. As the conditions under which multiple radical sites per chain are favored are also the conditions where the radical scavenging capacity deviates considerably from 100%, the number of radical sites per chain will be overestimated when assuming full scavenging capacity. As can be seen in Figure 1, the overestimation can be up to 20% for this system.

In Figure 2 the actual average number of radical sites per chain for the same systems and irradiation conditions

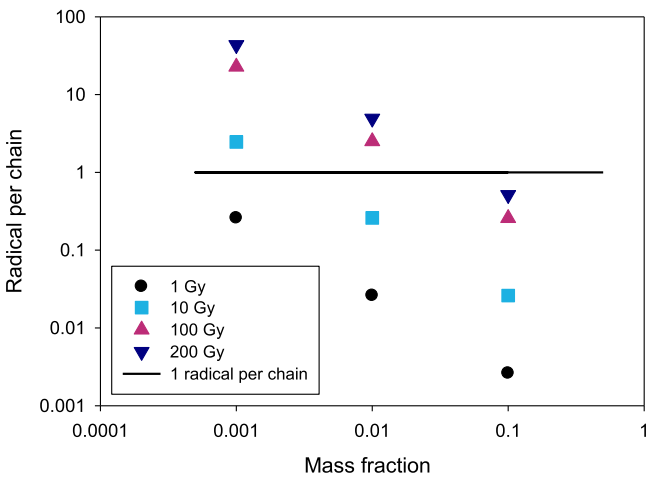

Figure 2. Average number of radical sites per chain plotted against polymer concentration (mass fraction).

presented in Figure 1 are illustrated. The average number of radical sites per chain is calculated from the ratio between total maximum radical concentration (concentration at the end of the electron pulse) and polymer concentration.

As can be seen, the average number of radical sites per chain is below one at all polymer concentrations for 1 Gy per pulse. For 10 Gy per pulse, the two highest polymer concentrations give average numbers of radicals per chain below one. For 100 and 200 Gy per pulse, only the highest polymer concentration results in less than one radical site per chain. For 10−200 Gy per pulse and the lowest polymer concentration (0.001 w/w) the average number of radical sites per chain ranges from 2.5 to 44. The corresponding range, calculated on the basis of 100% scavenging capacity, is 2.6−52 radical sites per chain, therefore very close to the simulations output.

The kinetics of the systems are illustrated in Figure 3a−c. The graphs show the total alkyl radical concentration as a

DOI: 10.1021/acs.jpca.9b03013
J. Phys. Chem. A XXXX, XXX, XXX−XXX

function of time at 100, 10, and 1 Gy per pulse for the three mass fractions considered in this study.

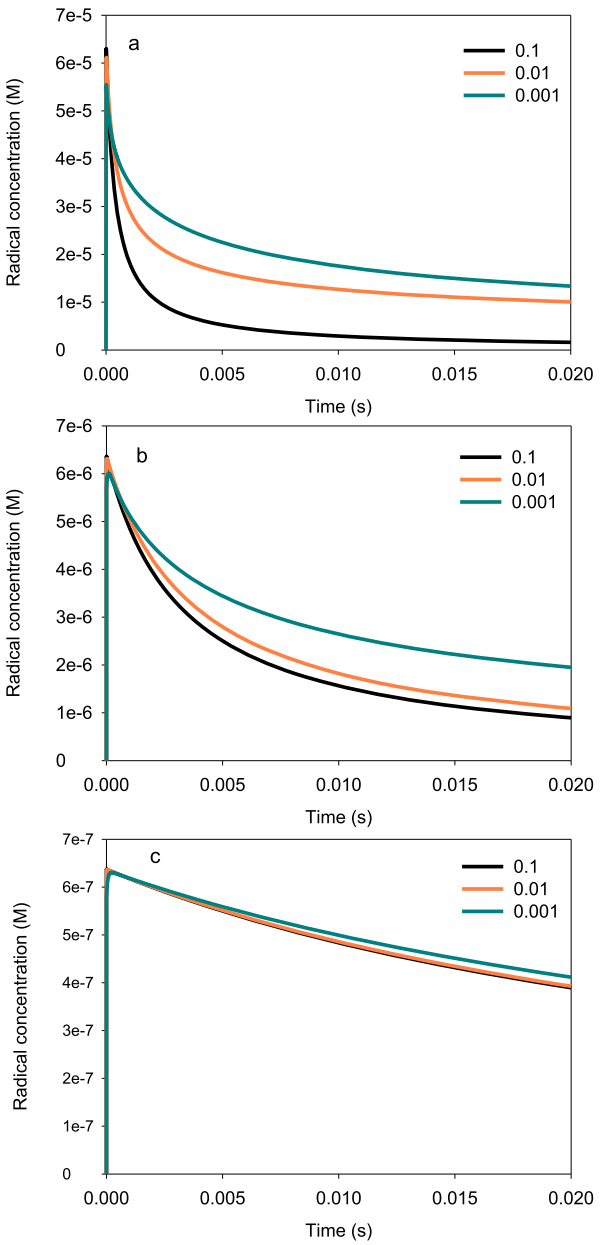

Figure 3. Total radical concentration as a function of time for 100 (a), 10 (b), and 1 Gy per pulse (c) for the polymer mass fractions 0.1 (black), 0.01 (orange), and 0.001 (green).

As can be seen, the radical decay is in general faster the higher the dose per pulse is. Indeed, this is to be expected for a system dominated by radical−radical reactions as a higher dose per pulse will give a higher initial radical concentration. However, even though the total maximum radical concentration at a given dose is virtually the same for all polymer mass fractions, the decay kinetics also depend on the polymer mass fraction. The mass fraction dependence decreases with decreasing dose per pulse. The general trend at the higher doses per pulse is that the radical decay is faster at higher polymer concentrations. In other words, the radical decay is faster when the radical sites are distributed over a larger number of molecules (i.e., at a lower average number of radical sites per chain). To analyze the kinetics of the systems presented in Figure 3 in more detail, in Figure 4 we have

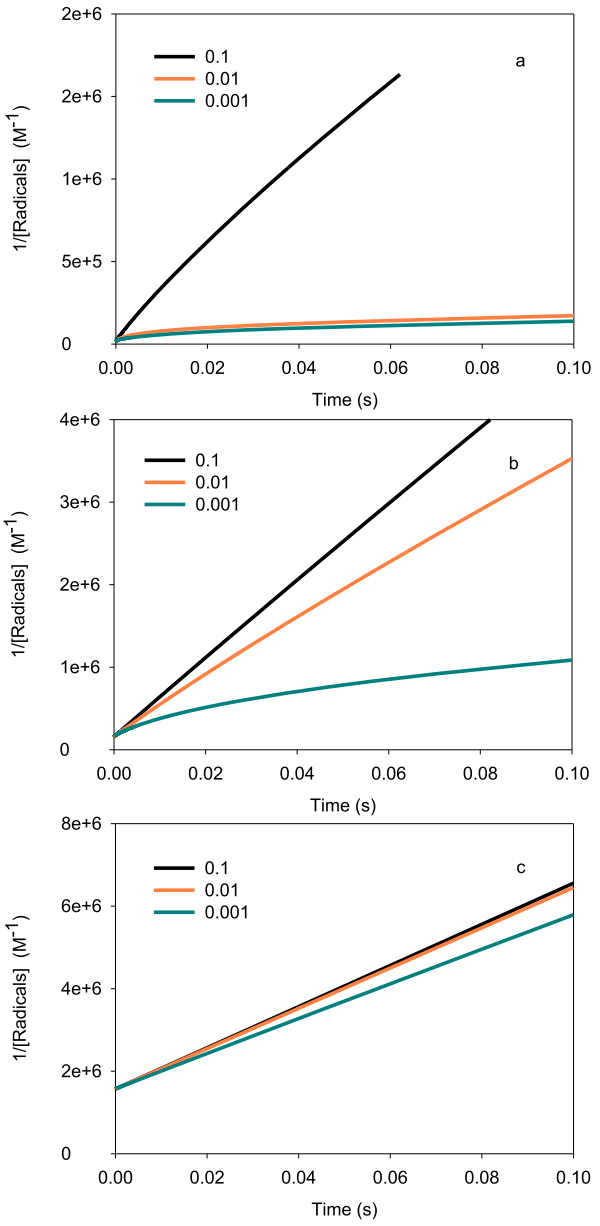

Figure 4. Inverse of the total concentration of radicals plotted against time for 100 (a), 10 (b), and 1 Gy per pulse (c) for the polymer mass fractions 0.1 (black), 0.01 (orange), and 0.001 (green).

plotted the inverse of the alkyl radical concentration against the reaction time after the pulse. For purely second-order kinetics, as in the case of an intermolecular radical−radical reaction between two molecules bearing one radical site each, a perfectly straight line is expected. When several radicals per chain are present, and intramolecular radical−radical reactions are expected, curved lines are observed and often analyzed in terms of dispersive kinetics.[23]

For the highest dose per pulse, we have not obtained a perfectly straight line at any of the polymer mass fractions. The slight deviation from linearity observed for the highest mass fraction would suggest the presence of chains bearing more than one radical site also for this system, although the average number of radicals per chain is below 1, as shown in Figure 2.

DOI: 10.1021/acs.jpca.9b03013
J. Phys. Chem. A XXXX, XXX, XXX−XXX

As the dose per pulse is decreased, the plots approach linearity at all polymer mass fractions.

Indeed, one would assume that all cases, where the average number of radical sites per chain is below one, display pure second-order kinetics, and that the rate constant obtained from Figure 4 is identical to the rate constant given in the model description above. However, when analyzing the seven cases where the average number of radical sites per chain is lower than one, it becomes clear that there is a certain contribution from multiple radical sites per chain also here. Even though the regression coefficient in a fit to second-order kinetics is 0.979 or higher, for the cases where the average number of radicals is below one, the rate constant obtained from the regression shows a clear dependence on the average number of radical sites per chain. This correlation is illustrated in Figure 5.

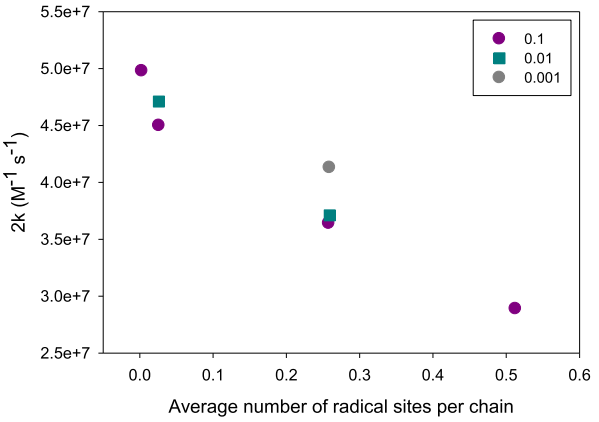

Figure 5. Second-order rate constant ($2k$) for the radical decay plotted against average number of radical sites per chain for the systems where the average number of radical sites per chain is below one according to Figure 2.

A slight effect of polymer concentration can also be observed. At a given average number of radical sites per chain, the second-order rate constant increases slightly with decreasing mass fraction of the polymer.

Monodisperse polymers are very uncommon and for this reason it is also interesting to explore the impact of molecular weight on the kinetics for radical−radical decay in the pulse-irradiated system. Simulations were performed for three different molecular weights (410, 41, and 4.1 kDa). In Figure 6, the total alkyl radical concentration is plotted against time for the three different molecular weights and for 100 and 1 Gy per pulse, respectively. The mass fraction of polymer is 0.001 in all cases.

As can be seen, the molecular weight has a major impact on the radical−radical decay kinetics at both the high and the low dose per pulse. At the higher dose per pulse, the molecular weight dependence can partly be attributed to the fact that we increase the number of radical-bearing chains as we decrease the molecular weight at a given mass fraction. As a consequence, bimolecular radical−radical reactions become increasingly important. For the lowest dose per pulse, the radical−radical decay is dominated by the bimolecular route already at the highest molecular weight. Hence, the observed molecular weight effect cannot be attributed to a change in the ratio between intra- and intermolecular radical−radical reaction. Instead, the difference in kinetics reflects the molecular weight effect on the rate constant for intermolecular radical−radical combination. At the higher dose per pulse, this effect also contributes to the observed difference in kinetics. It is interesting to note that intermolecular radical−radical combination becomes increasingly important at high doses per pulse as the molecular weight decreases at a given mass fraction.

Looking at this from the point of view of nanogel synthesis, we would expect low-molecular-weight fractions of the polymer to predominantly undergo intermolecular radical−radical combination, whereas the high-molecular-weight fractions will predominantly undergo intramolecular combination. The result would be a narrowing of the size distribution. Indeed, such a focusing effect has also been observed experimentally.[37] This was experimentally verified by a significant narrowing of the gel filtration chromatography peak upon irradiation of the polymer solution.

CONCLUSIONS

The new approach developed for numerical simulations of radiation-induced processes in aqueous polymer solutions yields results in fairly good agreement with experimental observations. The effects of molecular weight, polymer concentration, and dose per pulse on the kinetics of radical decay are all well reproduced by the model. In addition, the model confirms the experimentally observed limitations in scavenging capacity and provides an insight on the origin of the narrowing of molecular weight distribution in pulse-irradiated polymer solutions. These results encourage application of the model to even more complex irradiation conditions, when a train of short electron pulses are imparted to aqueous polymer

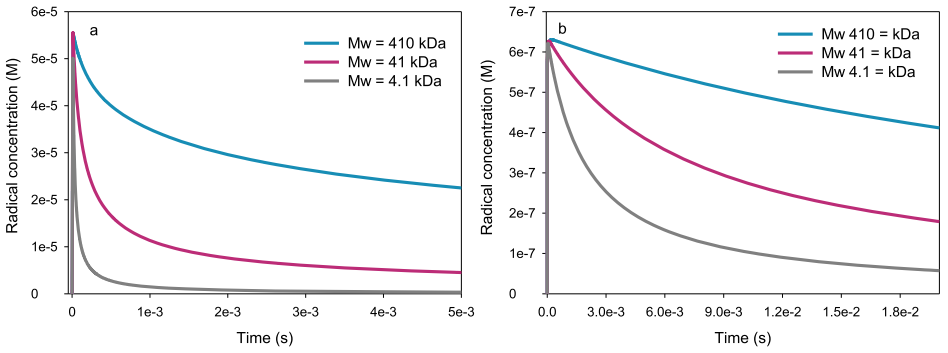

Figure 6. Total alkyl radical concentration as a function of time for three different molecular weights at 100 and 1 Gy per pulse, respectively.

DOI: 10.1021/acs.jpca.9b03013
J. Phys. Chem. A XXXX, XXX, XXX−XXX

solutions to deliver the higher doses required for nanogel synthesis.

AUTHOR INFORMATION

Corresponding Author

*E-mail: matsj@kth.se.

ORCID

Clelia Dispenza: 0000-0003-0076-5161

Mats Jonsson: 0000-0003-0663-0751

Notes

The authors declare no competing financial interest.

ACKNOWLEDGMENTS

B.D. acknowledges the Royal Institute of Technology for financial support. The IAEA CRP F22064 "Nanosized delivery systems for radiopharmaceuticals" is also acknowledged.

REFERENCES

(1) Soni, K. S.; Desale, S. S.; Bronich, T. K. Nanogels: an overview of properties, biomedical applications and obstacles to clinical translation. *J. Controlled Release* **2016**, *240*, 109−126.

(2) Englert, C.; Brendel, J. C.; Majdanski, T. C.; Yildirim, T.; Schubert, S.; Gottschaldt, M.; Windhab, N.; Schubert, U. S. Pharmapolymers in the 21st century: Synthetic polymers in drug delivery applications. *Prog. Polym. Sci.* **2018**, *87*, 107−164.

(3) Adams, G. E.; Posener, M. L.; Bisby, R. H.; Cundall, R. B.; Key, J. R. Free radical reactions with proteins and enzymes: the inactivation of pepsin. *Int. J. Radiat Biol Relat Stud. Phys Chem. Med.* **1979**, *35*, 497−507.

(4) Hawkins, C. L.; Davies, M. J. Generation and propagation of radical reactions on proteins. *Biochimica et Biophysica Acta—Bioenergetics* **2001**, *1504*, 196−219.

(5) Heinecke, J. W.; Li, W.; Francis, G. A.; Goldstein, J. A. Tyrosyl radical generated by myeloperoxidase catalyzes the oxidative cross-linking of proteins. *J. Clin. Invest.* **1993**, *91*, 2866−2872.

(6) Rosiak, J.; Schnabel, W. On the kinetics of polymer degradation in solution-XII. Radiolysis of poly(2,2,2-trichloroethyl methacrylate). *Eur. Polym. J.* **1984**, *20*, 1159−1163.

(7) Davis, J.; Sangster, D.; Senogles, E. Pulse radiolysis of aqueous solutions of N-vinylpyrrolidin-2-one and poly(N-vinylpyrrolidin-2-one). *Aust. J. Chem.* **1981**, *34*, 1423−1431.

(8) Ulanski, P.; Rosiak, J. M. Pulse radiolysis of poly(acrylic acid) in deoxygenated aqueous solution. *J. Radioanal. Nucl. Chem., Letters* **1994**, *186*, 315−324.

(9) An, J.-C.; Weaver, A.; Kim, B.; Barkatt, A.; Poster, D.; Vreeland, W. N.; Silverman, J.; Al-Sheikhly, M. Radiation-induced synthesis of poly(vinylpyrrolidone) nanogel. *Polymer* **2011**, *52*, 5746−5755.

(10) Beck, G.; Kiwi, J.; Lindenau, D.; Schnabel, W. On the kinetics of polymer degradation in solution-I. Laser flash photolysis and pulse radiolysis studies using the light scattering detection method. *Eur. Polym. J.* **1974**, *10*, 1069−1075.

(11) Ulański, P.; Janik, I.; Rosiak, J. M. Radiation formation of polymeric nanogels. *Rad. Phys. Chem.* **1998**, *52*, 289−294.

(12) Rosiak, J. M.; Ulański, P. Synthesis of hydrogels by irradiation of polymers in aqueous solution. *Rad. Phys. Chem.* **1999**, *55*, 139−151.

(13) Zainuddin, P. U.; Rosiak, J. M. Pulse radiolysis of poly(ethylene oxide) in aqueous solution. I. Formation of macroradicals. *Rad. Phys. Chem.* **1995**, *46*, 913−916.

(14) Ulański, P.; Zainuddin; Rosiak, J. M. Pulse radiolysis of poly(ethylene oxide) in aqueous solution. II. Decay of macroradicals. *Rad. Phys. Chem.* **1995**, *46*, 917−920.

(15) Kumar, V.; Bhardwaj, Y. K.; Sabharwal, S.; Mohan, H. The Role of Radiolytically Generated Species in Radiation-induced Polymerization of Vinylbenzyltrimethylammonium Chloride (VBT) in Aqueous Solution: Steady-state and Pulse Radiolysis Study. *J. Radiat. Res.* **2003**, *44*, 161−169.

(16) Ho, S. K.; Siegel, S.; Schwarz, H. A. Pulse radiolysis of polystyrene. *J. Phys. Chem.* **1967**, *71*, 4527−4533.

(17) Ogasawara, M.; Tanaka, M.; Yoshida, H. Reaction of solvated electron with poly(methyl methacrylate) and substituted poly(methyl methacrylate) in hexamethylphosphoramide studied by pulse radiolysis. *J. Phys. Chem.* **1987**, *91*, 937−941.

(18) Gelinck, G. H.; Warman, J. M. Charge Carrier Dynamics in Pulse-Irradiated Polyphenylenevinylenes: Effects of Broken Conjugation, Temperature, and Accumulated Dose. *J. Phys. Chem.* **1996**, *100*, 20035−20042.

(19) Behar, D.; Rabani, J. Pulsed radiolysis of poly(styrenesulfonate) in aqueous solutions. *J. Phys. Chem.* **1988**, *92*, 5288−5292.

(20) Cook, A. R.; Sreearunothai, P.; Asaoka, S.; Miller, J. R. Sudden, "Step" Electron Capture by Conjugated Polymers. *J. Phys. Chem. A* **2011**, *115*, 11615−11623.

(21) Ghaddar, T. H.; Wishart, J. F.; Kirby, J. P.; Whitesell, J. K.; Fox, M. A. Pulse radiolysis studies of dendritic macromolecules with biphenyl peripheral groups and a ruthenium tris-bipyridine core. *J. Am. Chem. Soc.* **2001**, *123*, 12832−12836.

(22) Spinks, J. W. T.; Woods, R. J. *An Introduction to Radiation Chemistry*; Wiley, 1990.

(23) Jeszka, J. K.; Kadlubowski, S.; Ulanski, P. Monte Carlo Simulations of Nanogels Formation by Intramolecular Recombination of Radicals on Polymer Chain. Dispersive Kinetics Controlled by Chain Dynamics†. *Macromolecules* **2006**, *39*, 857−870.

(24) Charlesby, A.; Alexander, P. Réticulation des polymères en solution aqueuse par les rayons gamma. *J. Chim. Phys. PCB* **1955**, *52*, 699−709.

(25) Alexander, P.; Charlesby, A. Effect of x-rays and γ-rays on synthetic polymers in aqueous solution. *J. Polym. Sci.* **1957**, *23*, 355−375.

(26) Sakurada, I.; Ikada, Y. Effects of gamma radiation on polymer in solution (IX): a turbidimetric study on solution of poly(vinyl alcohol) irradiated below critical concentration for gel formation (Special issue on physical, chemical and biological effects of gamma radiation, VII). *Bull. Inst. Chem. Res. Kyoto Univ.* **1996**, *44*, 66−73.

(27) Ulański, P.; Rosiak, J. M. The use of radiation technique in the synthesis of polymeric nanogels. *Nucl. Instrum. Methods Phys. Res. B* **1999**, *151*, 356−360.

(28) Dispenza, C.; Spadaro, G.; Jonsson, M. Radiation engineering of multifunctional nanogels. *Top. Curr. Chem.* **2016**, *374*, 69.

(29) Ditta, L. A.; Dahlgren, B.; Sabatino, M. A.; Dispenza, C.; Jonsson, M. The role of molecular oxygen in the formation of radiation-engineered multifunctional nanogels. *Eur. Polym. J.* **2019**, *114*, 164−175.

(30) Bartoszek, N.; Ulański, P.; Rosiak, J. M. Reaction of a low-molecular-weight free radical with a flexible polymer chain: Kinetic studies on the OH + poly(N-vinylpyrrolidone) model. *Int. J. Chem.Kin.* **2011**, *43*, 474−481.

(31) Rudakov, E. S.; Volkova, L. K.; Tretyakov, V. P. Low Selectivity reactions of OH radicals with alkanes in aqueous-solutions. *React. Kin. Catal. Lett.* **1981**, *16*, 333−337.

(32) Soylemez, T.; Schuler, R. H. Radiolysis of aqueous solutions of cyclopentane and cyclopentene. *J. Phys. Chem.* **1974**, *78*, 1052−1062.

(33) Borgwardt, V. U.; Schnabel, W.; Henglein, A. Pulsradiolytische messung der geschwindigkeitskonstanten der kombination von polyäthylenoxid-radikalen in wäßriger lösung. *Die Makromolekulare Chemie* **1969**, *127*, 176−184.

(34) Alfassi, Z. B. *General Aspects of the Chemistry of Radicals*; Wiley, 1999; p 584.

(35) Dahlgren, B. bjodah/polymer_radiolysis_pub: polymer_radiolysis_pub-1.0, version v1.0). Zenodo. http://doi.org/10.5281/zenodo.2579871 (Feb 28, 2019).

(36) Hindmarsh, A. C.; Brown, P. N.; Grant, K. E.; Lee, S. L.; Serban, R.; Shumaker, D. E.; Woodward, C. S. SUNDIALS: Suite of nonlinear and differential/algebraic equation solvers. *ACM Trans. Mathem. Softw.* **2005**, *31*, 363−396.

DOI: 10.1021/acs.jpca.9b03013
J. Phys. Chem. A XXXX, XXX, XXX−XXX

576 (37) Dispenza, C.; Sabatino, M. A.; Grimaldi, N.; Mangione, M. R.;
577 Walo, M.; Murugan, E.; Jonsson, M. On the origin of functionalization
578 in one-pot radiation synthesis of nanogels from aqueous polymer
579 solutions. *RSC Adv.* **2016**, *6*, 2582−2591.

DOI: 10.1021/acs.jpca.9b03013
J. Phys. Chem. A XXXX, XXX, XXX−XXX